Celestial Mechanics and Dynamical Astronomy (2021) 133:55
https://doi.org/10.1007/s10569-021-10054-4

ORIGINAL ARTICLE

Transfers from the Earth to L_2 Halo orbits in the Earth–Moon bicircular problem

José J. Rosales[1] · Àngel Jorba[1] · Marc Jorba-Cuscó[2]

Received: 3 July 2021 / Revised: 6 October 2021 / Accepted: 14 November 2021 /
Published online: 3 December 2021
© The Author(s) 2021

Abstract
This paper deals with direct transfers from the Earth to Halo orbits related to the translunar point. The gravitational influence of the Sun as a fourth body is taken under consideration by means of the Bicircular Problem (BCP), which is a periodic time dependent perturbation of the Restricted Three Body Problem (RTBP) that includes the direct effect of the Sun on the spacecraft. In this model, the Halo family is quasi-periodic. Here we show how the effect of the Sun bends the stable manifolds of the quasi-periodic Halo orbits in a way that allows for direct transfers.

Keywords Bicircular problem · Translunar point · Quasi-periodic Halo orbits · Invariant manifolds of tori · Earth–Moon transfers

1 Introduction

The translunar point, the L_2 point in the Earth-Moon Restricted Three Body Problem (RTBP), has interested researchers from the late sixties, Schmid and Center (1968). Since those first years, authors writing about the translunar point have in their sight the possibility of a permanent station on the lunar far side. Out of all the families that drive the dynamics nearby

This work has been supported by the Spanish grant PGC2018-100699-B-I00 (MCIU/AEI/FEDER, UE) and the Catalan Grant 2017 SGR 1374. The project leading to this application has received funding from the European Union's Horizon 2020 research and innovation programme under the Marie Skłodowska-Curie grant agreement #734557. J.J.R thanks Dr. Robert Pritchett for his comments on an earlier version of this paper. The authors thank the comments by the reviewers that helped to improve this manuscript.

✉ José J. Rosales
rosales@maia.ub.es

Àngel Jorba
angel@maia.ub.es

Marc Jorba-Cuscó
marc.jorba@unir.net

1 Departament de Matemàtiques i Informàtica, Universitat de Barcelona (UB), Gran Via de les Corts Catalanes 585, 08007 Barcelona, Spain

2 Universidad Internacional de la Rioja (UNIR), Av. de la Paz, 137, 26006 Logroño, Spain

the translunar point, a particular one has always stood out as the favorite, the Halo family (see Farquhar 1970). The main reason is the geometry of the orbits within the family as they are always visible from the Earth. This property allows permanent communication with a spacecraft following a Halo orbit. A remarkable part of the efforts during these decades has been devoted to the problem of constructing a path from the Earth to a Halo orbit. That is, designing a transfer orbit for the spacecraft to depart from the Earth and inject onto the Halo orbit.

Mathematically speaking, the Halo family is a family of periodic orbits of the RTBP that appears from a pitchfork bifurcation as the horizontal and vertical Lyapunov family merge (see Jorba and Masdemont 1999). As periodic orbits, the trajectories in the Halo family have a linear behaviour that encodes their stability property in the eigenvalues of the monodromy matrix. In particular, the members of the standard Halo family have linear behaviour of type center × saddle; this is, a pair of imaginary eigenvalues conjugated to each other corresponding to the center, and a real eigenvalue and its inverse corresponding to the saddle. The other two eigenvalues are equal to 1 due to the autonomous character of the RTBP Hamiltonian, and are associated to the manifold defined by the family of Halo orbits. This implies that each of these orbits have one stable and one unstable manifold that are tangent to the stable and unstable eigenspaces of the linearized system around the orbit. These stable and unstable manifolds provide connections with different parts of the phase space and one can take advantage of this fact to build transfer orbits.

The use of invariant manifolds to transport (and control) a spacecraft to a target orbit was first analyzed in Gómez et al. (2001) and it has been extensively studied in the context of the RTBP for both the Sun-Earth system, and the Earth-Moon system. For the Halos around the L_1 point of the Sun-Earth system the invariant manifolds are especially interesting because, depending on the geometry and size of the Halo orbit, the stable manifold passes close to the Earth. In this case, a spacecraft in a parking orbit can be inserted in the stable manifold of a target Halo orbit with only one maneuver performed at the intersection of parking orbit with the stable manifold. Once the spacecraft is in the manifold, it coasts to the orbit associated with that manifold with no need to perform extra maneuvers[1]. In the Earth-Moon RTBP, unfortunately, this is not the case (see Bernelli Zazzera et al. 2004; Alessi et al. 2010). Different approaches have been developed for the Earth-Moon system, and these in general require two or more maneuvers. These approaches, along with representative references, are outlined in Sect. 2.3.

The Earth-Moon RTBP, however, does not take into account the gravitational pull of the Sun. It has been shown, in a number of papers, that solar gravitation plays an important role in the Earth-Moon environment and that its inclusion as a perturbation of the Earth-Moon RTBP leads to significant changes in the phase space. See (Simó et al. 1995; Castellà and Jorba 2000; Jorba 2000) for results regarding specifically the triangular points, Jorba et al. (2020) for the case of L_1 and Jorba and Nicolás (2020, 2021) for the case of L_3. Moreover, the case of the translunar point has been tackled in Alessi et al. (2012), Rosales et al. (2021).

The main goal of this paper is to study this effect in the transfer from a parking orbit around the Earth to the Halo family related to the translunar point. A natural question arising from this context is whether the change on the phase space of the Earth-Moon RTBP produced by the Sun is sufficient to bring the invariant manifolds of the Halo orbits close to the Earth, allowing for one-maneuver transfers. During this paper we will see that the answer is positive.

[1] This statement is valid from a theoretical point of view, where maneuver execution is perfect and instantaneous, the position and velocity of the spacecraft at the maneuver time is known with no error, and the spacecraft is considered massless. In practice, however, none of these assumptions are true, and usually it is required to perform small correction maneuvers.

There are, of course, several ways to model the influence of the Sun's gravity in the Earth-Moon system. In this study, we focus on the Bicircular Problem (BCP), Huang (1960), Cronin et al. (1964). It is, broadly speaking, a pair of coupled RTBP (details on the construction of the model are provided in Sect. 2.1). The BCP can be written as a periodic time perturbation of the RTBP. Notice that this means that the dimension of the phase space is increased by one. Also the invariant objects increase their dimension: the Lagrangian points no longer exist as equilibria but they are replaced by periodic orbits with the same period as the perturbation (in fact, in some cases the perturbation produced by the Sun is large enough to produce bifurcations). An analogous situation holds for periodic orbits: they become, generically, two dimensional quasi-periodic orbits, gaining the frequency of the perturbation (Jorba and Villanueva 1997). In particular, the translunar Halo family is composed of quasi-periodic orbits in the BCP. Therefore, in this paper, we use invariant manifolds attached to quasi-periodic orbits to build the transfers.

The paper is structured as follows: Sect. 2 is devoted to preliminaries. In there, we introduce specific details on the BCP and provide a description of relevant aspects of the Halo family in this model. The preliminaries end with Sect. 2.3, in which we provide a summary of different approaches to compute transfers. In Sect. 3 we construct transfer orbits from a parking orbits about the Earth to Quasi-Periodic Halo orbits in the BCP. Finally, in Sect. 4 we provide our conclusions and future work.

2 Preliminaries

In this section we review some previous results and techniques that have been used in the paper. In particular, we focus on a description of the model and the basic ideas for the transfer.

2.1 The Sun–Earth–Moon Bicircular model

A key aspect of the present work is to account for the gravitational pull of the Sun upon the spacecraft. The effect of the Sun is twofold: first there is the direct effect, i.e., the pull that the spacecraft receives directly from the Sun. Second, the indirect effect, i.e., the different attraction on the spacecraft coming from the different motion of the Earth and the Moon due to the effect of the Sun on the Earth and the Moon. To get a clear insight of the dynamical aspects of the problem one should select the simplest models among the ones that contain the desired phenomena. As we will see in this case the considered model includes the effect of the Sun in a quite simple way, that is, as a periodic time dependent perturbation of the Restricted Three Body Problem (RTBP). When perturbing the RTBP periodically, the complexity of the phase space increases, that is, the dimension of the invariant objects is increased, generically, by one. This is a well-known fact that, moreover, is developed with more detail in Sect. 2.2. As we will be dealing with a periodic time dependent perturbation of the RTBP, we devote some words on recalling some basic properties of the latter.

The RTBP is a model that describes the motion of a massless particle under the gravitational influence of two masses (the primaries). In the simplest of its versions the two primaries revolve along circular orbits about their common barycentre. It is standard to use specific units so that the distance between the primaries is equal to one, the sum of their masses is equal to one and their period of revolution is equal to 2π. With these units the universal gravitational constant is also equal to one. Moreover, it is also standard to consider a rotational frame of reference (the synodic frame), fixing the two primaries in the horizontal axis. With

Table 1 Values of the parameters of the BCP

$\mu = 0.012150581623$	$m_s = 328900.55$
$\omega_s = 0.925195985518$	$a_s = 388.811143023351$

these conditions, the motion of an infinitesimal particle under the gravitational attraction of the primaries is described by a three degrees of freedom Hamiltonian system,

$$H_{RTBP} = \frac{1}{2}(p_x^2 + p_y^2 + p_z^2) - xp_y + yp_x - \frac{1-\mu}{r_{PE}} + \frac{\mu}{r_{PM}}, \tag{1}$$

where $r_{PE}^2 = (x-\mu)^2 + y^2 + z^2, r_{PM}^2 = (x-\mu+1)^2 + y^2 + z^2$ and $\dot{x} = p_x + y, \dot{y} = p_y - x$, $\dot{z} = p_z$. The constant μ is called the mass parameter and represents the non-dimensional mass of the smallest primary. In the case of the Earth-Moon system, the smallest primary is the Moon and has a mass $\mu \approx 0.012$.

The BCP is among the simplest versions of the Restricted Four Body Problem. It is assumed that two of the primaries (Earth and Moon) revolve around their common center of mass and, at the same time, the barycentre of these two bodies and a third primary (Sun) revolve also along circular orbits around the barycentre of the third primary and the barycentre of the first two. The BCP is the study of the motion of an infinitesimal particle under the attraction of these three masses. Notice that the motion of these masses is not coherent, that is, the trajectories prescribed for the primaries do not follow Newton's laws. While this could be seen as inconvenient, the BCP has been used to successfully describe relevant aspects of the dynamics of the real Earth-Moon system, see (Simó et al. 1995; Jorba 2000; Jorba and Nicolás 2020).

As a dynamical system, the BCP is a three and a half degrees of freedom Hamiltonian system or, equivalently, it has three degrees of freedom and a periodic time dependence. When written in the standard RTBP frame and units, the dynamics of the BCP is governed by the following Hamiltonian function,

$$H = \frac{1}{2}(p_x^2 + p_y^2 + p_z^2) - xp_y + yp_x - \frac{1-\mu}{r_{PE}} - \frac{\mu}{r_{PM}} - \frac{m_S}{a_S^2}(y\sin\vartheta - x\cos\vartheta) - \frac{m_S}{r_{PS}}. \tag{2}$$

Here, the quantities μ, r_{PE} and r_{PM} are the ones appearing in (1). The constant m_S denotes the mass the of Sun, a_S is the averaged semi-major axis of the Sun, $\vartheta = \omega_S t$, ω_S is the frequency of the Sun in the RTBP synodic frame, $T_S = \frac{2\pi}{\omega_S}$ is its period and $r_{PS}^2 = (x - a_S\cos\vartheta)^2 + (y - a_S\sin\vartheta)^2 + z^2$. The value of these constants are given in Table 1.

Notice that the Hamiltonian function of the BCP (2) is the Hamiltonian of the RTBP (1) plus two extra terms, the first corresponds to the Coriolis term due to the motion of the Earth-Moon barycentre and the second one associated to the gravitational effect of the Sun.

2.2 The neighborhood of the translunar point

In the context of the RTBP, it is a very well-known fact that the translunar point L_2 is an equilibrium point of type saddle×centre×centre. For each elliptic direction, there exists a family of periodic orbits such that:

- It is tangent to the elliptic eigensubspace at L_2,
- near L_2, it can be locally parameterized by the frequency,

- as the members of the family get close to the equilibrium point, their frequencies tend to the corresponding normal mode (the frequency given by the complex eigenvalue) of the equilibrium point.

These families are known as the Lyapunov families of periodic orbits. As the linear behaviour of the translunar point is saddle×centre×centre, there are two Lyapunov families that are born at the point, one contained in the (x, y) plane and named the horizontal Lyapunov family, and one born in the (z, p_z) direction and called the vertical Lyapunov family. Both families are, near L_2, of center×saddle type. The planar family, at some distance of L_2 undergoes a pitchfork bifurcation that produces a new family, the so-called Halo orbits (this description remains true for the collinear points L_1 and L_3).

When a time-dependent periodic perturbation (such as the influence of the Sun's gravity introduced in the BCP) is considered, the translunar point is replaced by a periodic orbit with the same period as the perturbation (this is a consequence of the Implicit Function Theorem and these kinds of orbits are known as dynamical equivalents). When the perturbation is not small, this picture can change. In the BCP, the influence of Sun's gravity is strong enough to produce bifurcations and, in particular, merge the dynamical equivalent of L_2 and a resonant Lyapunov orbit with half the period of the Sun. In particular, there is no direct replacement of L_2 in the BCP.

The effect that the periodic perturbation has on the periodic orbits that populate the neighborhood of the translunar point is analogous to the one on the point itself but much more complicated. Periodic orbits, generically, gain a frequency and become invariant tori with two frequencies (the one of the periodic orbit plus the one of the perturbation). More generally, invariant tori of any dimension gain the frequency of the Sun, see (Jorba and Villanueva 1997). The last statement is not true whenever one of the frequencies of the unperturbed tori are a rational multiple of the frequency of the Sun.

In Rosales et al. (2021), the authors study the effect of the Sun's gravity on the neighborhood of the translunar point of the BCP. In particular, the most relevant families (horizontal and vertical Lyapunov families and the Halo one) are considered. Notice that these classical families of periodic orbits of the RTBP become, in the BCP, families of two-dimensional invariant tori. Special attention is given to the Halo family. In particular, two different two-dimensional families of Halo-like invariant tori, labeled as Type I and Type II, are shown to exist in the aforementioned work. The Type I family is the family that replaces the classic Halo family of the RBTP in the BCP. Type II family comes from a 1:2 resonant Quasi-Halo orbit: that is, a family of two-dimensional tori which is locally tangent to the elliptic eigenspace of the main Halo family that has $\omega_S/2$ as one of its inner frequencies. Representative examples of a member of each of these families can be found in Fig. 1.

2.3 Approaches to compute transfers

In this section we review some of the main techniques to transfer a spacecraft from a parking orbit to Halo or Lissajous orbits around L_1/L_2. This is not meant to be an exhaustive review of the literature, but a short overview of the main approaches. These techniques have been mainly divided into two groups, with a main focus on transfers from a parking orbit around the Earth to a Halo orbit around L_2.[2] These are summarized in the following paragraphs:

- Direct Transfer: This approach is a purely ballistic transfer, and it requires two maneuvers: one to leave the parking orbit, and the second one to insert the spacecraft in the target

[2] A similar argument applies to L_1, but for the sake of clarity, we focus our attention on L_2.

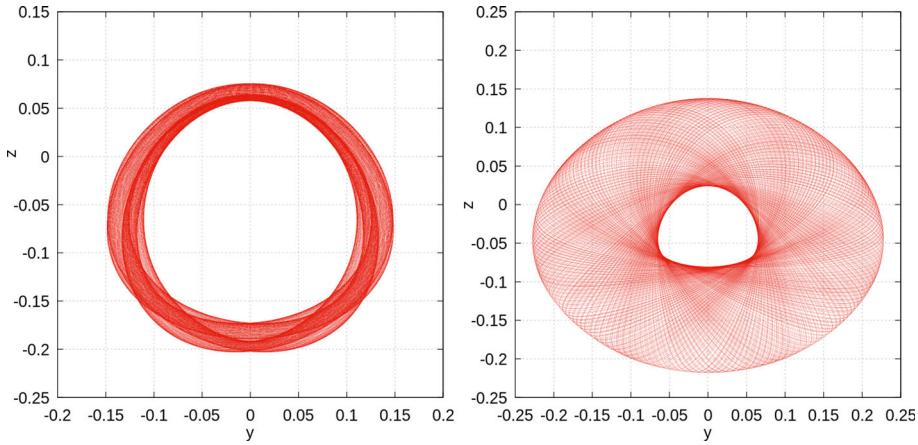

Fig. 1 Examples of members of the Type I and Type II families. Left: Projection of a member of Type I family onto the plane y-z. Right: Projection of a member of Type II Family onto the plane y-z

orbit. This approach requires, in general, an expensive maneuver to leave the Earth (approximately 3300–3500 m/s), and a less expensive maneuver, but still relatively big to insert into the Halo orbit (500–700 m/s). The main benefit of this approach is that the time of travel spans between 4 and 13 days. Previous works that document this approach can be found in Rausch (2005), Le Bihan et al. (2014).

- Invariant manifolds: This approach uses the invariant manifold of the target Halo orbit to provide a low-cost transfer. The use of invariant manifolds has been proved to be useful in the Sun-Earth system, where the invariant manifolds get very close to the sphere of influence of the Earth. Hence, to insert a spacecraft from a parking orbit to the target orbit is relatively cheap. However, in the Earth-Moon system the invariant manifolds of the Halo orbits do not pass close to the Earth. In order to try to take advantage of the natural dynamics of the system provided by the invariant manifolds, in Bernelli Zazzera et al. (2004) the authors develop an algorithm for the solution of the Lambert's three-body problem that leaves the transfer time free and tries to minimize the cost of the insertion maneuver in the invariant manifold. That is, they target a point in the invariant manifold that requires minimum fuel expenditure, and not its associated Halo orbit. Once on the invariant manifold, the spacecraft coasts to the target Halo orbit. The total cost of these transfers from a LEO orbit varies between 3100 and 3200 m/s with a transfer time between 40 and 255 days. Another implementation of the use of invariant manifolds can be found in Alessi et al. (2010), Li and Zheng (2010). In Alessi et al. (2010) the author computes transfers from a LEO orbit to a square Lissajous orbit around L_1 or L_2. The Δv costs documented in Alessi et al. (2010) are also in the 3000–4000 m/s range. In Li and Zheng (2010) the authors study indirect transfers to the L_1 libration point with a three-maneuver approach with a total cost of 3439.8 m/s and a travel time of 22.9 days.

The interested reader in transfers from the Earth to the Moon is referred to Parker and Anderson (2014), where the authors survey thousands of low-energy transfers form the Earth to different orbits around the Moon.

Note that all of the above approaches are either limited to the Earth-Moon RTBP, or consider the decoupled Sun-Earth RTBP and Earth-Moon RTBP. Thus, the contribution of the Sun's gravitational effect either is completely neglected, or it is considered only partially

during specific parts of the transfer. As mentioned in the previous section, the approach taken here accounts directly for the effect of the Sun's gravity as modeled in the BCP model. The numerical experiments and the results are discussed in Sect. 3.

2.4 The stroboscopic map

As it has been mentioned before, the BCP is a model that depends periodically on time. To cope with this kind of models it is standard to use the so-called stroboscopic map P_{T_S} which is defined, for an initial condition of the phase space at time $t = 0$, as the flow evaluated at time T_S. Periodic orbits of period T_S appear as fixed points of the stroboscopic map. In a similar way, the two-dimensional invariant tori whose one of their frequencies is ω_S, appear as invariant curves. In the following sections, we focus on several members of Type I and Type II families of quasi-periodic orbits that are treated as invariant curves.

3 Transfers in the BCP

In this section we study the transfer from parking orbits around the Earth to three Type I Halo orbits, and three Type II Halo orbits in the BCP. The only parameters fixed in the parking orbit are the semi-major axis and the eccentricity. The semi-major axis is set to be equal to the radius of the Earth, $R_E = 6400$ km, plus 200 km. We define $R = R_E + 200$. The eccentricity is set equal to zero. That is, we consider the family of circular orbits around the Earth traveling at approximately 200 km above the Earth's surface. This family can be interpreted as a sphere with center in the center of the Earth, and radius equal to the radius of the Earth plus 200 km. From now on, we will refer to this sphere as the LEO sphere.

Note that for practical applications we would also be concerned about the inclination of the parking orbit. Ideally, the inclination should be close to the latitude of the launching facility. For this analysis, this has been intentionally omitted given that the main focus is to study whether or not, in the BCP, the invariant manifold of the Halo-like orbits considered here intersect with the LEO sphere.

The idea is the following: given a target Halo-like orbit (Type I or Type II), a suitable mesh of initial conditions on the stable manifold are integrated backward in time. When one of these trajectories intersects the LEO sphere, then a valid transfer is considered to exist. In that event, the Δv between the parking orbit in the LEO sphere corresponding to the intersection point, and the corresponding point in the unstable manifold is computed. This gives an initial measure of the total Δv transfer cost. The total transfer time Δt is also recorded, as well as longitude and latitude of the intersection point in the LEO sphere. The latitude gives a first approximation of the parking orbit inclination. The computation of the Δv and Δt are given in physical units (km/s and days, respectively).

3.1 The stable manifold

To get a local representation of the potential transfers we use a parametrization of the linear approximation of the stable manifold close to the invariant curve: if $\theta \in [0, 2\pi)$ parametrizes the invariant curve and h is a small real value, the linear approximation to the stable manifold is

$$p_0^s(h, \theta) = \mathbf{x}(\theta) + h\psi_s(\theta), \tag{3}$$

where $\mathbf{x}$ is a parameterization of the invariant curve, ψ_s is the eigenfunction associated to the stable eigenvalue λ_s (see Rosales et al. 2021 for the computation of ψ_s and λ_s). The value h is selected such that $|h| < h_0/|\lambda_s|$, for a fixed value $h_0 \in \mathbb{R}^+$ such that $h_0/|\lambda_s|$ is small (for example, on the order of 10^{-6} or 10^{-7}), so that the error of this approximation is $O(h_0^2)$. Positive and negative values of h correspond to each of the two sides of the manifold. From now on, we will refer to the *positive* (resp. *negative*) side of the manifold as the side generated with a $p_x > 0$ for $p_0^s(0)$, and a positive (resp. negative) value of h. For reference, the positive side is in the direction towards the Moon from the invariant curve.

Roughly speaking, a fundamental set of a manifold is a set of initial conditions on the manifold such that the orbits starting there generate, forward and backward in time, the full manifold. In this case, and for the stroboscopic map, the fundamental sets are cylinders. As $\lambda_s > 0$, given a positive real number h_0 we can define a fundamental cylinder for the linear approximation (3) as the set of points corresponding to $[h_0, h_0/\lambda_s] \times [0, 2\pi)$. If h_0 is small enough, this is a good approximation to a fundamental cylinder of the manifold. Note that, in this case, the circle at the bottom $\{h_0\} \times [0, 2\pi)$ is mapped to the top circle of the cylinder $\{h_0/\lambda_s\} \times [0, 2\pi)$ by the inverse of the stroboscopic map.

Once we have defined the fundamental cylinder, we create a grid of $N \times N$ points on $[0, 2\pi) \times [h_0, h_0/\lambda_s]$. The value of h_0 has been selected such that

$$\max_i \left(\| P_T^{-1}(\mathbf{x}(\theta_i)) - \mathbf{x}(\theta_i - \rho) - \frac{h_0}{\lambda_s} \psi_s(\theta_i - \rho) \| \right) < \delta, \quad \theta_i = \frac{2\pi \cdot i}{N}, \quad i = 0, ..., N-1,$$

where $P_{T_s}^{-1}$ is the inverse of the stroboscopic map at time T_s, T_s is the period of the Sun in the normalized frame, and ρ is the rotation number of the associated invariant curve. For this analysis we used $N = 2000$ and $\delta = 10^{-6}$.

Then, we integrate this initial data backward in time to span the stable manifold, and check whether or not these trajectories intersect with the LEO sphere. Moreover, we check collisions with the Moon, and for trajectories that leave the sphere of influence of the Earth-Moon system. For the latter, we stop the integration if the distance to the Earth-Moon barycentre exceeds at any point during the integration 6 units of distance in the normalized frame. This is equivalent to approximately 2.3 million kilometers. Of course, we also need to set a maximum integration time. For this analysis, the maximum integration time was set to $6T_s$. This corresponds to approximately 191.5 days of physical time. We acknowledge that this number is somewhat arbitrary, but it is justified in the sense that we are looking for reasonable transfer times.

As a summary, we have defined a fundamental cylinder on the linear approximation of the stable manifold that is very close to the invariant curve, we have chosen a mesh of points on this fundamental cylinder and we have integrated them backward in time looking for one of the following four events:

1. The stable manifold intersects the LEO sphere.
2. The stable manifold collides with the Moon.
3. The stable manifold leaves the sphere of influence of the Earth-Moon system; this is, the distance of the computed state to the Earth-Moon barycentre exceeds 6 times the distance from the Earth to the Moon.
4. After $6T_s$ units of time in the normalized frame, none of the above occur (these will be referred to wandering trajectories).

As has been mentioned before, for this analysis we have chosen three Type I and three Type II quasi-periodic Halo orbits around the L_2 point of the BCP and run the process described in the previous paragraphs. The projections of the invariant curves of the three

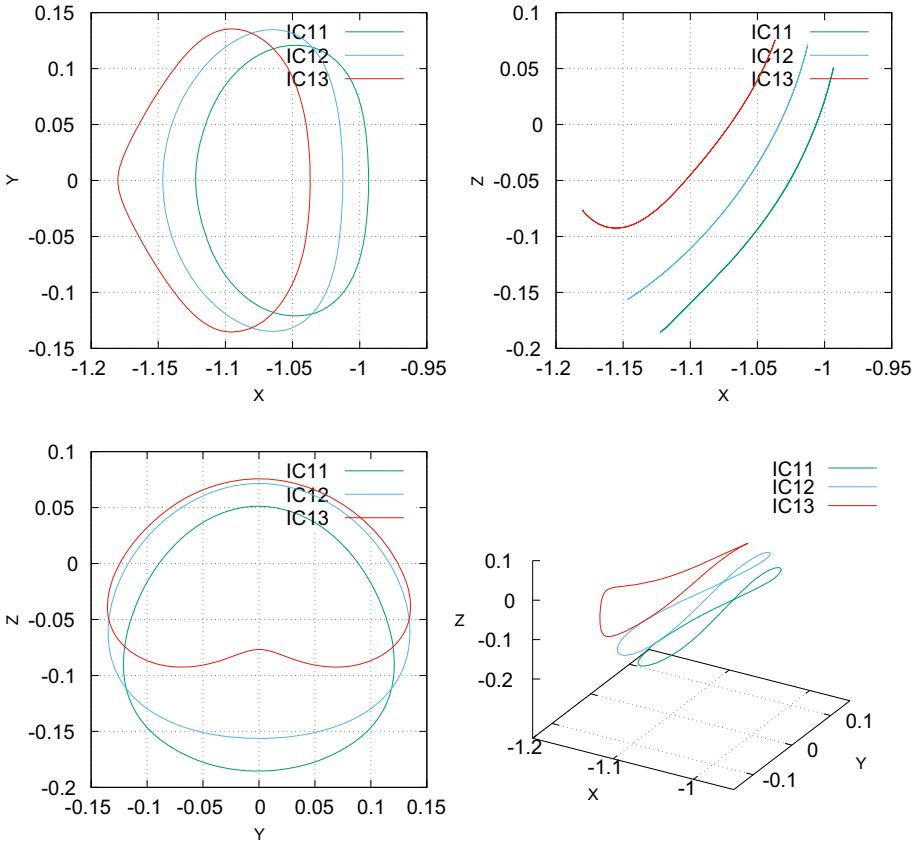

Fig. 2 Invariant curves IC11, IC12, IC13 of the family of Type I orbits in the BCP

Type I orbits are shown in Fig. 2. These are referred as IC11 (green), IC12 (blue), and IC13 (red). The three corresponding of the Type II are in Fig. 3. These are labeled as IC21 (green), IC22 (blue), and IC23 (red). Note that the invariant curves IC21 and IC23 in Fig. 3 are very close to each other (not only in position space, but also in the sense that the difference between their rotation numbers is small). These were intentionally chosen to assess the sensitivity in the transfers with respect to the distance of target orbits. Tables 2 and 3 contain the rotation number associated to each of the trajectories selected and the unstable eigenvalues.

The results of the analysis are shown in Figs. 4 and 5 . The color code is the following: red corresponds to those trajectories on the unstable manifold that intersect with the LEO sphere; green denotes trajectories that collide with the Moon; yellow the trajectories that escape the Earth/Moon sphere of influence; and black the trajectories that do not meet any of the previous criteria. The horizontal axis corresponds to the angle associated with a point on the invariant curve. The vertical axis corresponds to the signed height of the fundamental cylinder, where the sign denotes the side of the manifold. As a general comment that applies to both Figs. 4 and 5, notice that all figures are periodic with respect to the horizontal axis (this is, the left side of the plot matches with the right side). About the vertical axis note that, by construction, the bottom and top rows are related by the stroboscopic map at time equal to the period of the Sun, T_s. For the sake of clarity, let's consider the positive side of the manifold.

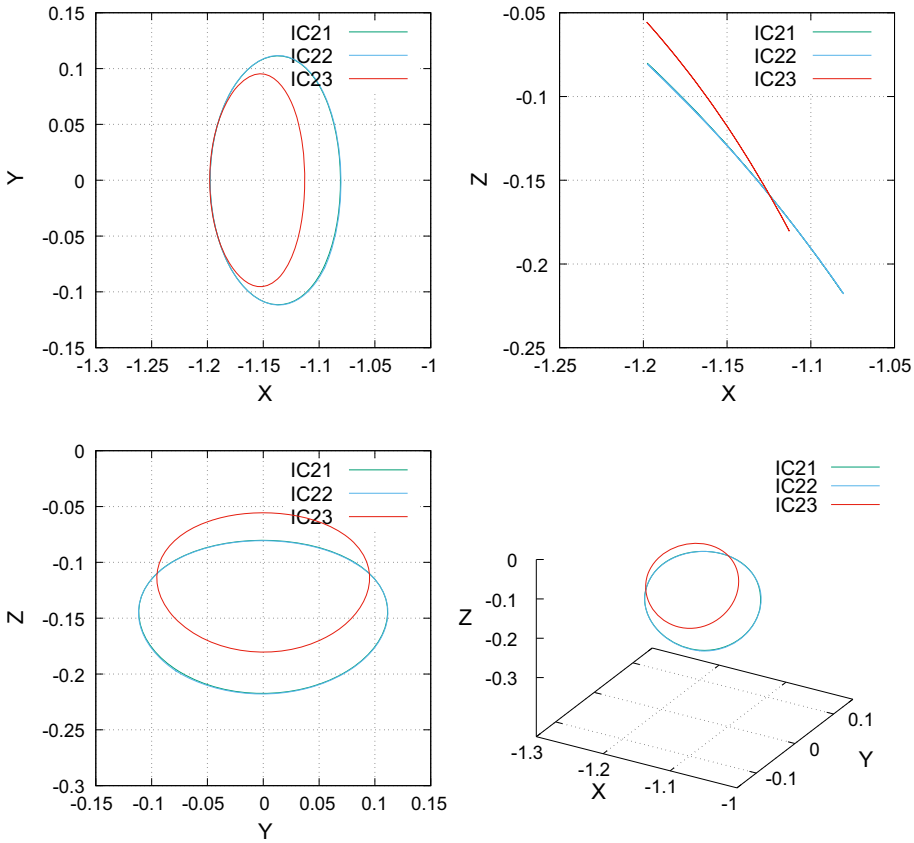

Fig. 3 Invariant curves IC21, IC22, IC23 of the famliy of Type II orbits in the BCP

Table 2 Type I invariant curves characteristics

Invariant curve	Rotation number	$\lambda_s^{-1} = \lambda_u$
IC11	3.239814740891185	1407.242345974658
IC12	1.658983813333736	19619.97458514797
IC13	0.645906459334160	179352.0342756758

Table 3 Type II invariant curves characteristics

Invariant curve	Rotation number	$\lambda_s^{-1} = \lambda_u$
IC21	3.097097182626015	24082.25237481578
IC22	3.128958892611009	23104.95771489475
IC23	2.085220044971505	93487.30771525634

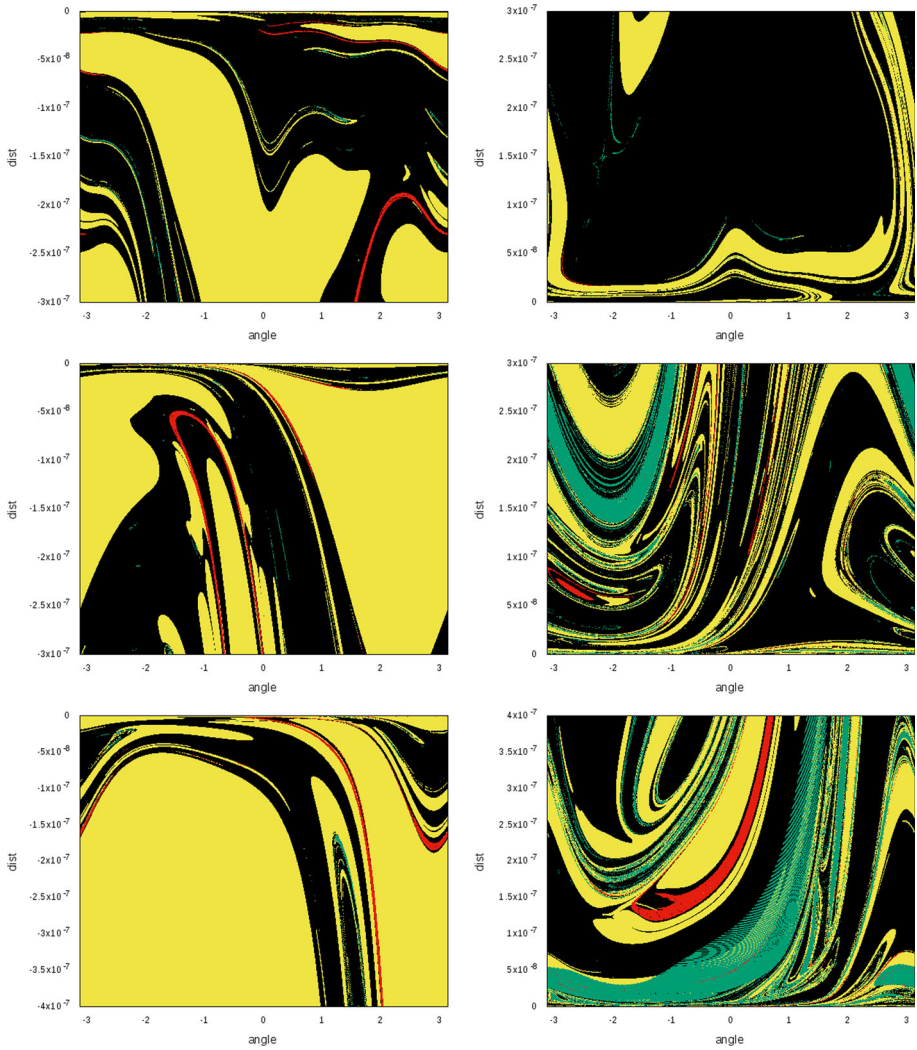

Fig. 4 Fundamental cylinders for Type I orbits. Valid transfers are colored in red, trajectories where a particle leaves the Earth/Moon system are colored in yellow, collisions with the Moon are green, and none of the previous cases in black. See text for details

The bottom row corresponds to the trajectories obtained fixing $h = \min([h_0, h_0/\lambda_s]) = h_0$, and changing the angle $\theta \in [0, 2\pi)$. The top row corresponds to the trajectories associated with $h = \max([h_0, h_0/\lambda_s]) = h_0/\lambda_s$, where λ_s is the eigenvalue corresponding to the stable component of the hyperbolic part. By construction, the top row is the image of the bottom row by the stroboscopic map. With that, it would be expected that the top row is equal to the bottom one plus a shift equal to the rotation number of the invariant torus under consideration (see, for example, Jorba and Nicolás 2020). Looking at Figs. 4 and 5 this is clearly not the case. The reason is that we are using a total integration time equal to $6T_s$, and this is relatively short. Using a short integration time has the following effect: when we integrate backward an initial condition on the stable manifold at distance h_0 from the invariant curve, we check

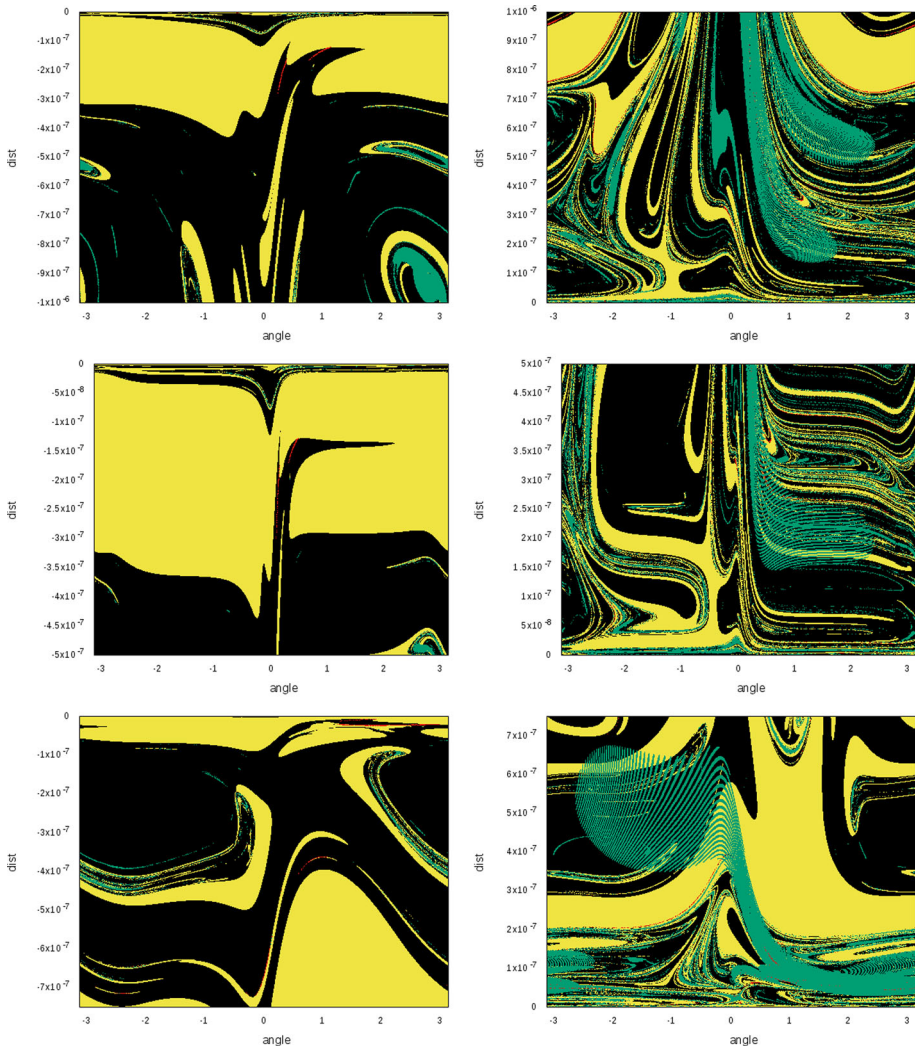

Fig. 5 Fundamental cylinders for Type II orbits. Valid transfers are colored in red, trajectories where a particle leaves the Earth/Moon system are colored in yellow, collisions with the Moon are green, and none of the previous cases in black. See text for details

for events that happen in that period of time (intersection with the LEO sphere, collision with the Moon, escape, or none of the previous). When we repeat this process for the initial conditions of the top row, we know that these are the image of the initial conditions of the bottom row. In other words, it is as if we have already integrated a total of T_s units of time. Hence, the results of the top row are the same as if we integrated $7T_s$ units of time the initial conditions of the bottom row. This may cause that the events we observe are different for the bottom and top rows. If we were to integrate an infinite (or a large enough) amount of time, we would observe that shift.

3.2 Transfer trajectories

The first row in Fig. 4 contains the results for the invariant curve IC11, the second row for the invariant curve IC12, and the third one for the invariant curve IC13. The first column is the negative side of the stable manifold, and the second one the positive side. For both the positive and negative sides of the manifold, the distance from the invariant curves as defined in at the beginning of this section (this is, the value h_0/λ_s) is equal to 3×10^{-7} units of distance in the normalized coordinates (or approximately 115 m) for IC11 and IC12, and equal to 4×10^{-7} units of distance in the normalized frame (or approximately 150 m) for IC13.

It is observed that in all cases except of the IC11, positive side case, there are small regions (colored in red) where the stable manifold intersects the LEO sphere. For the IC11, positive side case, there are also connections via the stable manifold, but there are not clearly perceived in the image. In all cases the dominant outcomes are either when the particle leaves the Earth-Moon sphere of influence (colored in yellow) or it follows a wandering trajectory for the time-span integrated (colored in black). In all cases there are also collisions with the Moon (regions colored in green). It is in the cases IC12 and IC13, positive side in both cases, where there are large regions where the stable manifold collides with the Moon (recall that the positive side of the manifold is the one oriented towards the Moon). It also noted that the closest the target orbit is to the Moon, the more collisions exist (in this order, for farthest to closest: IC11, IC12, and IC13).

The scenario for the Type II trajectories is captured in Fig. 5. The first row contains the results for the invariant curve IC21, the second row for the invariant curve IC22, and the third one for the invariant curve IC23. As for the Type I case, the first column is the negative side of the stable manifold, and the second one the positive side. The distances from the invariant curves in this case are 10^{-6} units of distance in the normalized frame (or approximately 380 m) for IC21, 5×10^{-7} units of distance in the normalized frame (or approximately 190 m) for IC22, and 7×10^{-7} units of distance in the normalized frame (or approximately 270 m) for IC23. In all cases these values are for both the positive and negative sides of the manifold.

In this case, there are very few transfers that intersect with the LEO sphere, and these are barely noticeable in the figures. For the case of the invariant curves IC21, IC22, and IC23, there are almost no trajectories of the unstable manifold that intersect the LEO sphere. In the negative side there are small regions where the trajectories collide with the Moon, while in the positive side there are quantitatively more (again, this is the side oriented towards the Moon). Most of the trajectories, either leave the Earth-Moon's sphere of influence, or wander around during the total time of the integration.

3.3 Transfer costs

For each one of the cases analyzed, the transfers that minimize three different cost functions have been computed. These three cost functions are, as mentioned before:

- $J_1(\theta, h) = \Delta v(\theta, h)$
- $J_2(\theta, h) = \Delta t(\theta, h)$
- $J_3(\theta, h) = \sqrt{\Delta v(\theta, h)^2 + \Delta t(\theta, h)^2}$

When doing this analysis, it is important to define how the Δv was computed, and what is meant by "transfer time" and how it was calculated. The total Δv was computed the same way as in Alessi et al. (2010). This is, if $\hat{\mathbf{v}}$ is velocity of the spacecraft when it intersects with the LEO sphere, the first step is to convert this vector from conjugated momentum to synodic

velocity. Let us call this velocity $\mathbf{v}$. Note that in theory we should also convert this velocity from the rotating frame to the inertial frame. However, because this transformation does not change the module of the vector, we can skip it. With that, the Δv is computed as follows,

$$\Delta v = \sqrt{\|\mathbf{v}\|^2 + v_s^2 - 2\|\mathbf{v}\| \cos\left(\frac{\pi}{2} - \beta\right)},$$

where β is the angle between the velocity vector $\mathbf{v}$ and the normal to the LEO sphere. The value v_s is the module of the velocity of a circular orbit on the LEO sphere, and it is computed using the *vis-viva* equation,

$$v_s = \sqrt{\frac{1-\mu}{R}}.$$

Note that as the LEO sphere is close to the Earth, it is natural to assume a Keplerian motion for the parking orbit.

The computation of the total transfer time is a matter of convention. Note that, in theory, if we follow stable manifold, the total time needed to arrive to the invariant curve is infinite. This is because the dynamics on the stable manifold tends asymptotically to the invariant curve. However, for practical purposes we define a threshold such that if the distance to the invariant curve is below it, we consider the transfer completed. This threshold is (within reason) arbitrary, and here we have chosen a distance equal to $D = 100$ km as a threshold. The next question is how to estimate time t_D at which the particle will be a distance D to the invariant curve. This is not as straightforward as computing the distance between two points in space. The approach we took to estimate the time t_D is to use the linear flow in a vicinity of the invariant curve. Let us define

$$\bar{\lambda} = \frac{\log \lambda_s}{T_s}.$$

This value $\bar{\lambda} < 0$ is the eigenvalue associated with the flow on the stable manifold near the invariant curve, and it is a measure of the rate at which, locally, an initial condition close to the invariant curve approaches the curve or, if the time goes backwards, the rate at which an orbit on the manifold departs. The evolution of the distance d to the invariant curve can be modeled, at first order, by the differential equation $\dot{d} = \bar{\lambda} d$. Then, the time needed to go between distances h and D is given by

$$t_D = \frac{1}{\bar{\lambda}} \log\left(\frac{D}{h}\right).$$

Hence, if T is the total time of integration from the distance h to the invariant curve, and t_D the time to reach a distance equal to D, the total transfer time Δt is defined as

$$\Delta t = T - t_D.$$

This is the time reported in the rest of the section with, again, a value of $D = 100$ km.

The results for each case, for a parking orbit traveling at 200 km above the Earth's surface, are summarized in Table 4 for Type I orbits, and in Table 5 for Type II orbits. The first column of Tables 4 and 5 states the invariant curve associated with the target orbit, the second column is the manifold side (positive/negative), the third the cost function minimized, the fourth and fifth columns the Δv and the total transfer time Δt associated to the cost function, and the last column the latitude of the intersection point in the LEO sphere.

Looking at the results in Table 4 it is observed that the cheapest transfer in terms of Δv corresponds to the case $\{\text{IC13}, -, J_1\}$ (meaning: IC13 invariant curve, negative side of the

Table 4 Transfer cost to Type I Halo orbits

Invariant curve	Manifold side	Cost function	Δv (km/s)	Δt (days)	Latitude (deg)
IC11	+	J_1	3.2669	142.0661	13.439409
IC11	–	J_1	3.1641	138.3457	12.037744
IC11	+	J_2	4.0805	141.6628	-5.295561
IC11	–	J_2	3.2158	118.6235	1.816246
IC11	+	J_3	3.5347	141.9145	1.483374
IC11	–	J_3	3.2158	118.6235	1.816246
IC12	+	J_1	3.1970	124.5192	-7.529808
IC12	–	J_1	3.2180	122.3772	8.693360
IC12	+	J_2	6.4304	113.8526	11.245034
IC12	–	J_2	4.3185	112.5306	-28.175822
IC12	+	J_3	6.4304	113.8526	11.245034
IC12	–	J_3	4.3185	112.5306	-28.175822
IC13	+	J_1	3.1734	110.3284	-3.869638
IC13	–	J_1	3.1617	141.6146	-5.502472
IC13	+	J_2	3.2671	110.3107	-7.639184
IC13	–	J_2	3.3344	100.2958	7.040290
IC13	+	J_3	3.1734	110.3284	-3.869638
IC13	–	J_3	3.3344	100.2958	7.040290

invariant manifold, and J_1 cost function) with a total of 3.1617 km/s. This transfer, however, takes almost 142 days to reach the target orbit. In terms of total transfer time, the cheapest corresponds to the cases {IC13, –, J_2} and {IC13, –, J_3} with slightly over 100 days. For this option, the total cost terms of Δv is 3.3344 km/s, making this transfer very reasonable. It is a good idea to look at other options that are a trade-off between a cheap maneuver and a reasonable transfer time. In these category, we have the cases {IC13, +, J_1}, and {IC13, +, J_3}, where the total Δv cost is 3.1734 km/s, and the total travel time is around 110 days. This provide a saving of around 161 m/s at the expense of an increase in travel time of approximately 10 days. Another important aspect is the latitude at the LEO sphere. In all the cases, the latitudes are below 7.1 degrees, which is also a reasonable value.

Table 5 shows some transfers for Type II Halo orbits. In this scenario, the case {IC23, –, J_1} is the cheapest transfer in terms of Δv with a total of 3.1231 km/s, and a total transfer time of around 132 days to reach the target orbit. The shortest transfers in this case are {IC23, –, J_2} and {IC23, –, J_3}, with a total transfer time of approximately 104 days, but with a total Δv cost of more than 4.1 km/s. As the in the case for the Type I case, we can look for trade-offs. However, after looking at the data, it seems that the option that minimizes the total Δv is the best, given the low latitude intersection with the LEO sphere, and how the total transfer time compares with the other options.

Overall, and as a main takeaway, it can be concluded that there are transfers in the BCP comparable in total Δv and transfer time with other techniques such as the Indirect Transfer, but with the main advantage that only one maneuver is required.

Let us have a closer look at the IC13 case. Figure 6 shows the trajectory followed by the transfer {IC13, –, J_2}. This trajectory corresponds to the stable manifold of the target orbit IC13; this is, is the trajectory that a spacecraft would follow after departing from the Earth to

Table 5 Transfer cost to Type II Halo orbits

Invariant curve	Manifold side	Cost function	Δv (km/s)	Δt (days)	Latitude (deg)
IC21	+	J_1	3.1841	161.5869	5.645610
IC21	–	J_1	3.2668	152.9112	-8.222948
IC21	+	J_2	5.1727	127.4293	-24.409394
IC21	–	J_2	3.3851	144.9792	-18.574485
IC21	+	J_3	4.3772	127.8258	-31.131620
IC21	–	J_3	3.3851	144.9792	-18.574485
IC22	+	J_1	3.4450	170.1543	-0.049602
IC22	–	J_1	3.2184	153.3855	5.282887
IC22	+	J_2	8.9775	132.5925	66.012057
IC22	–	J_2	3.5173	145.8660	-22.626341
IC22	+	J_3	5.3619	133.2474	13.593364
IC22	–	J_3	3.5173	145.8660	-22.626341
IC23	+	J_1	4.1184	122.0862	-17.195273
IC23	–	J_1	3.1231	132.0245	9.329800
IC23	+	J_2	6.0772	121.4934	27.102303
IC23	–	J_2	4.1081	104.1051	-11.507359
IC23	+	J_3	3.1744	124.6729	-7.456677
IC23	–	J_3	4.1081	104.1051	-11.507359

the target orbit. It can be seen that the trajectory circles the Earth and the Moon twice before converging to the target orbit. This 'bending' of the invariant manifold is due to the direct gravitational effect of the Sun.

Figure 7 shows different zoomed projections of the transfer to the target orbit. The black circle corresponds to the radius of the Moon, and blue circle to the LEO sphere (this is, the radius of the Earth plus 200 km). It can be seen that for the IC13 orbit there is no Moon occultation. This is relevant because for communications purposes it is important that the Earth-Satellite line-of-sight is not blocked by the Moon.

Moreover, and for the sake of completeness, it is interesting to see how the different parameters computed during the analysis relate to each other. For example, from the data collected we can see how the Δv changes as a function of the total transfer time. This is shown in Fig. 8a for the IC13 case. It is observed that there is a concentration of transfer trajectories that take less than 125 days, and that there are relatively cheap transfers that take a long time. Also, it can be observed that the total maneuver cost is between 3.1617 km/s (the minimum computed in this case) and slightly more than 13 km/s. Finally, it is interesting to observe that the minimum Δv transfers are not the ones with maximum time, which is a usual trade-off.

Another interesting plot is total Δv as function of the latitude at which the transfer intersects with the LEO sphere. Figure 8b displays that information again for the IC13 scenario, and shows that the majority of the transfers with less than 4 km/s are concentrated between a latitude of $-20°$ and $40°$. It also shows that transfers to low latitudes exhibit a wider range of Δv values.

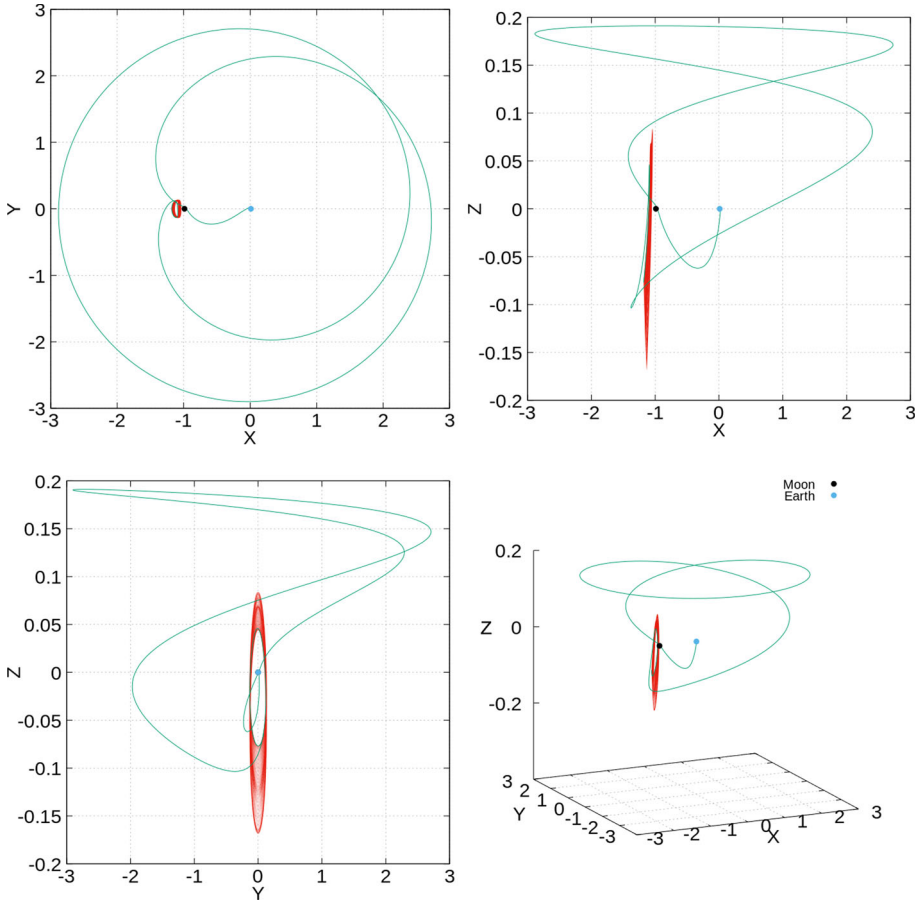

Fig. 6 Trajectory followed by the transfer {IC13, –, J_2}

4 Conclusions and further work

In this work we have studied the potential use of invariant manifolds attached to quasi-periodic Halo orbits to coast from the Earth to the neighborhood of the translunar point. A relevant aspect of our study is the consideration of the Sun's gravitational pull as well as the effect of the Earth and the Moon, that is, we have addressed the problem with a restricted four body problem approach.

We have based the study on the use of the BCP model, a non-coherent and simple model that assumes a bicircular motion for the Sun, the Earth and the Moon. The BCP can be written as a periodic time dependent perturbation of the classical RTBP. In this context, the classical Halo orbits gain, generically, the frequency of the perturbation becoming two-dimensional invariant tori. Following the nomenclature of Rosales et al. (2021), we have labeled these two-dimensional tori as Halo orbits of Type I. On the other hand, the two-dimensional quasi-periodic Halo orbits of the RTBP whose frequency is resonant with the one of the Sun, remain two-dimensional tori once the perturbation is turned on. Those orbits are named, also according to Rosales et al. (2021), as Halo orbits of Type II.

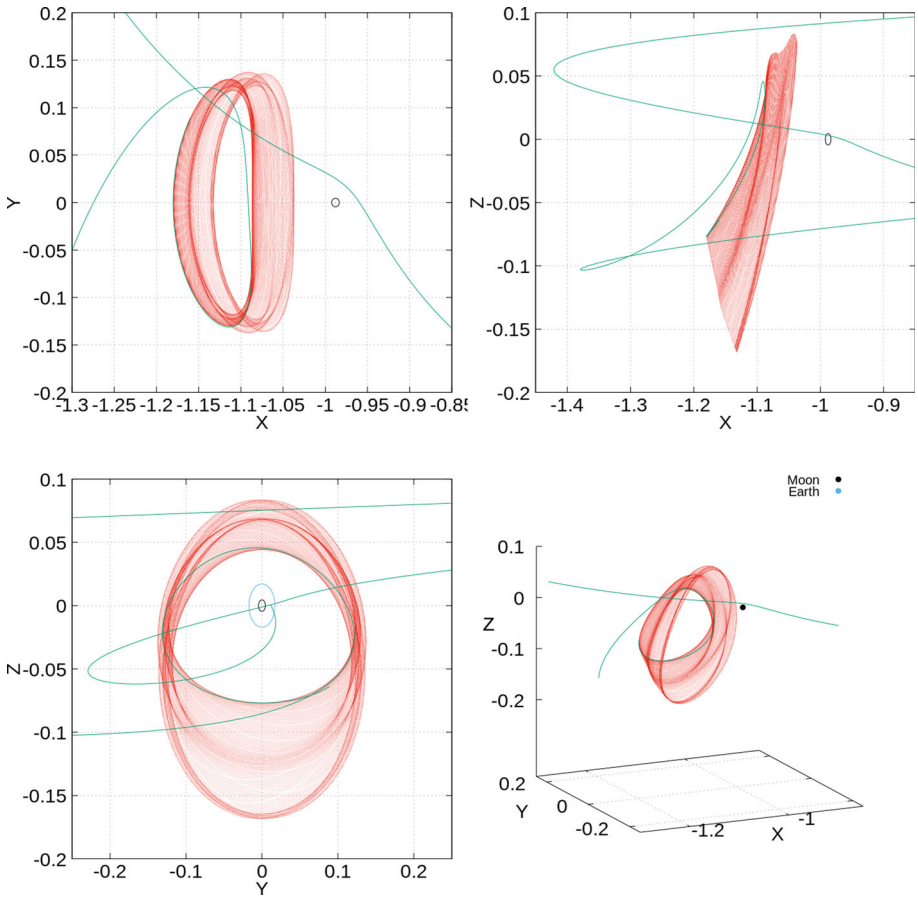

Fig. 7 Zoom around the target orbit trajectory followed by the transfer {IC13, –, J_2}

The strategy has been to compute the stable manifold of several Halo orbits of Type I and Type II of the BCP noticing that there are some parts of those manifolds that intersect with the LEO sphere of parking orbits around the Earth. Then, one-maneuver transfers are designed where the total cost comes from the insertion into a parking orbit of 200 km above the Earth. We would like to remark that this kind of single maneuver transfers have never been shown to exist in the RTBP. Therefore, the Sun gravity is an essential ingredient for modeling these trajectories. Moreover, in all cases, it has been shown that the total cost, in terms of Δv and transfer time, is comparable to other techniques requiring two or more maneuvers.

Further steps along this line of research would include the demonstration that these transfers can be transitioned to higher fidelity models, and to better understand the trade-offs between Δv and total transfer times.

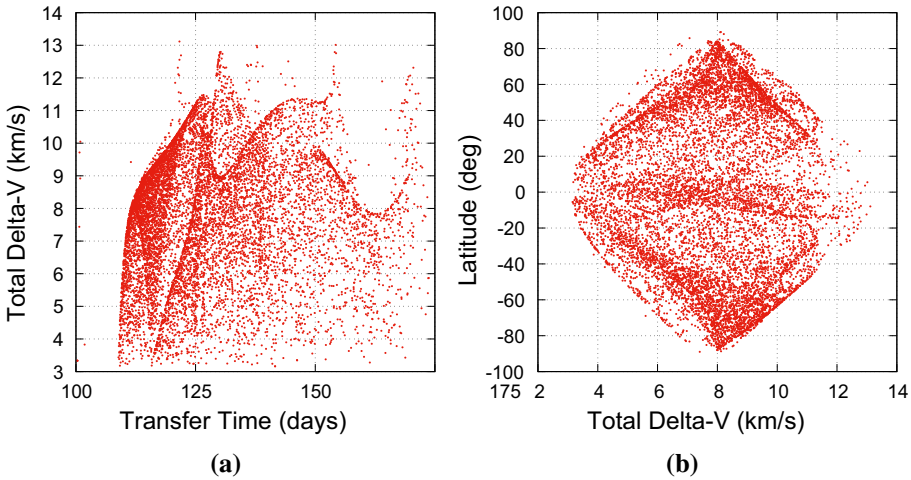

Fig. 8 Plots of transfer time against total Δv (left) and Δv against latitude in the LEO Sphere (right) for the IC13 case

Funding Open Access funding provided thanks to the CRUE-CSIC agreement with Springer Nature.

Declarations

Conflict of interest The authors declare that they have no conflict of interest.

Open Access This article is licensed under a Creative Commons Attribution 4.0 International License, which permits use, sharing, adaptation, distribution and reproduction in any medium or format, as long as you give appropriate credit to the original author(s) and the source, provide a link to the Creative Commons licence, and indicate if changes were made. The images or other third party material in this article are included in the article's Creative Commons licence, unless indicated otherwise in a credit line to the material. If material is not included in the article's Creative Commons licence and your intended use is not permitted by statutory regulation or exceeds the permitted use, you will need to obtain permission directly from the copyright holder. To view a copy of this licence, visit http://creativecommons.org/licenses/by/4.0/.

References

Alessi, E.M., Gómez, G., Masdemont, J.J.: Two-manoeuvres transfers between LEOs and Lissajous orbits in the Earth-Moon system. Adv. Space Res. **45**(10), 1276–1291 (2010)

Alessi, E.M., Gómez, G., Masdemont, J.J.: Further advances on low-energy lunar impact dynamics. Commun. Nonlinear Sci. Numer. Simul. **17**(2), 854–866 (2012)

Bernelli Zazzera, F., Topputo, F., Massari, M.: Assessment of mission design including utilisation of libration points and weak stability boundaries (03–4103b). Technical report, European Space Agency (2004)

Castellà, E., Jorba, À.: On the vertical families of two-dimensional tori near the triangular points of the bicircular problem. Celestial Mech. **76**(1), 35–54 (2000)

Cronin, J., Richards, P.B., Russell, L.H.: Some periodic solutions of a four-body problem. Icarus **3**, 423–428 (1964)

Farquhar, R.W.: The Control and Use of Libration-point Satellites. NASA TR R, National Aeronautics and Space Administration (1970)

Gómez, G., Llibre, J., Martínez, R., Simó, C.: Station keeping of libration point orbits. ESOC contract 5648/83/D/JS(SC), final report, European Space Agency, 1985. Reprinted as *Dynamics and mission*

design near libration points. Vol. I, Fundamentals: the case of collinear libration points, volume 2 of World Scientific Monograph Series in Mathematics, (2001)

Huang, S.S.: Very restricted four-body problem. Technical note TN D-501. Goddard Space Flight Center, NASA (1960)

Jorba, À., Jorba-Cuscó, M., Rosales, J.J.: The vicinity of the Earth-Moon L_1 point in the Bicircular Problem. Celestial Mech. **132**(2), 11 (2020)

Jorba, À., Masdemont, J.: Dynamics in the center manifold of the collinear points of the restricted three body problem. Physica D **132**, 189–213 (1999)

Jorba, À., Nicolás, B.: Transport and invariant manifolds near L_3 in the Earth-Moon Bicircular model. Commun. Nonlinear Sci. Numer. Simulat. **89**, 105327 (2020)

Jorba, À., Nicolás, B.: Using invariant manifolds to capture an asteroid near the L_3 point of the Earth-Moon Bicircular model. Preprint (2021)

Jorba, À.: A numerical study on the existence of stable motions near the triangular points of the real Earth-Moon system. Astron. Astrophys. **364**(1), 327–338 (2000)

Jorba, À., Villanueva, J.: On the persistence of lower dimensional invariant tori under quasi-periodic perturbations. J. Nonlinear Sci. **7**(5), 427–473 (1997)

Le Bihan, B., Kokou, P., Receveu, J.-B., Lizy-Destrez, S.: Computing an optimized trajectory between Earth and an EML2 halo orbit. In: AIAA Guidance, Navigation, and Control Conference, National Harbor, MD, USA (2014)

Li, M., Zheng, J.: Indirect transfer to the Earth-Moon L_1 libration point. Celest. Mech. Dyn. Astron. **108**, 203–213 (2010)

Parker, J., Anderson, R.: Low-Energy Lunar Trajectory Design. Wiley, New York (2014)

Rausch, R.R.: Earth to Halo Orbit Transfer Trajectories. Purdue University, Indiana (2005).. (**Master's thesis**)

Rosales, J.J., Jorba, À., Jorba-Cuscó, M.: Families of Halo-like invariant tori around L_2 in the Earth-Moon Bicircular Problem. Celest. Mech. Dyn. Astron. **133**, 03 (2021)

Schmid, P.E., Center, Goddard Space Flight.: United States. National Aeronautics, and Space Administration. Lunar Far-side Communication Satellites. NASA TN D-4509. National Aeronautics and Space Administration (1968)

Simó, C., Gómez, G., Jorba, À., Masdemont, J.: The Bicircular model near the triangular libration points of the RTBP. In: Roy, A.E., Steves, B.A. (eds.) From Newton to Chaos, pp. 343–370. Plenum Press, New York (1995)

Publisher's Note Springer Nature remains neutral with regard to jurisdictional claims in published maps and institutional affiliations.